Available online at www.sciencedirect.com
ScienceDirect
Journal of Power Sources 161 (2006) 640–647
JOURNAL OF POWER SOURCES
www.elsevier.com/locate/jpowsour

# Overcharge studies of carbon fiber composite-based lithium-ion cells

S. Hossain *, Y.-K. Kim, Y. Saleh, R. Loutfy

*LiTech, LLC, 7960 S. Kolb Road, Tucson, AZ 85706, USA*

Received 6 April 2006; received in revised form 21 April 2006; accepted 21 April 2006
Available online 5 June 2006

**Abstract**

Prototype lithium-ion pouch cells of 5.5 Ah have been fabricated with carbon fiber composite anodes, $LiCoO_2$ cathodes, and $LiPF_6$ electrolyte to investigate the overcharge characteristics of these cells at the 1*C* rate. The cells were made with anode to cathode capacity (A/C) ratios of 1.0 and 1.1. The cells were first examined for charge–discharge characteristics at different rates in order to determine the delivered capacity, specific energy and energy density and rate capability, and to ensure that the cells are suitable for overcharge studies. The current, voltage, and temperature responses during overcharge to 12 V were recorded. Maximum temperatures of 65 and 85 °C were observed with the cells with A/C equal to 1.1 and 1.0, respectively. The overcharged cells were dissected in an inert atmosphere and their components were analyzed using scanning electron microscopy and x-ray fluorescence spectroscopy. It is believed that a relatively low amount of heat is generated with carbon fiber composite-based lithium-ion cells and a separator shutdown mechanism is operative in the cell system which prevents fire or explosion during overcharge.


*Keywords:* Carbon fiber composite; Lithium-ion battery; Overcharge; Anode–cathode ratio; Heat generation; Shut-down mechanism

## 1. Introduction

Lithium-ion batteries are widely used in portable electronic devices. Their lack of safety when operated under abusive conditions, however, prevents other avenues of application. One of the most important safety issues for the present state-of-the-art lithium-ion batteries is related to overcharge, which can lead to thermal runaway and ultimately to fire or explosion of the batteries. To protect a battery from overcharge, the lithium-ion battery industry uses a number of safety measures, such as overcharge protection circuits, positive temperature coefficient resistors, pressure sensitive rupture disks, temperature sensitive separators, etc. The use of these safety devices not only increases the cost of lithium-ion batteries but also lowers their specific energy and energy density. For small capacity and relatively low voltage batteries, the above measures to protect the battery and users are found to be acceptable. For high capacity, multi-cell high voltage batteries, such as are being considered for military, aerospace, and vehicular applications, a battery chemistry that is resistant to abusive conditions, such as overcharge is desirable so that if the battery is accidentally exposed to overcharge due to electronic malfunction, there still will not be any safety concerns.

Several complex energy-related processes are involved during overcharge of a lithium-ion cell:

(a) Electrical energy due to injected current is released which may: (i) increase cell temperature, (ii) decompose electrolyte solvent(s), (iii) dissolve cathode material, (iv) deposit metallic lithium on the carbon anode, (v) shrink separator, etc.
(b) Heat energy associated with undesirable side-reactions of: (i) anodes and (ii) cathodes is released.
(c) Dissipation of heat energy from the cell to the ambient environment occurs.

The difference in the heat energy gains and losses determine whether the heat that remains within the cell is rising or falling and this determines the ultimate fate of the overcharged cells. If a lithium-ion cell is designed and developed in such a way that the total retained heat energy is sufficiently low so that it does not trigger thermal runaway, overcharge-related safety incidents can be avoided. One can, therefore, address the overcharge related safety issues by using one or a combination of the following approaches:

* Corresponding author. Tel.: +1 520 574 1980; fax: +1 520 574 1983.
*E-mail address:* shossain@mercorp.com (S. Hossain).

0378-7753/$ – see front matter © 2006 Elsevier B.V. All rights reserved.
doi:10.1016/j.jpowsour.2006.04.111

(a) Increasing the exposed surface area of the cell so that most of the generated heat energy can dissipate to the ambient environment.
(b) Eliminating/minimizing side-reactions that generate heat.

Present day applications, however, often require compact cell design and, therefore, step (a) is rarely acceptable. The battery scientists are, therefore, in search of a cell chemistry that provides step (b).

There have been a number of papers published on the side-reactions that generate heat from lithiated anodes [1–6] and delithiated cathodes [3,5,7] during cell temperature rise. From accelerated rate calorimetry (ARC) measurements of a lithiated carbon anode, Richard and Dahn [2,4] showed two exotherms—the first one corresponded to the decomposition of a metastable SEI layer at around 100 °C and the second exotherm at around 150 °C was due to the reaction of $LiC_x$ with the electrolyte. For both the exotherms, the amount of heat generation depends on the surface area of the carbon anode—the higher the surface area, the higher the heat generation. It has been shown that the reactions of lithiated carbon with PVDF binder [3,8] are exothermic. MacNeil and Dahn [7] investigated the thermal decomposition of $Li_{0.5}CoO_2$ using accelerated rate calorimetry and X-ray diffraction (XRD) and concluded that loss of oxygen from $Li_{0.5}CoO_2$ occurs only above 200 °C. The involvement of the cathode in a safety incident during overcharge, therefore, occurs only if the cell temperature is close to 200 °C. Takeuchi and co-workers [9] concluded from their overcharge studies of 1.5 Ah cells that the $Li_xCoO_2/Li_yC_6$ system itself can produce the high temperature reactions that lead to rupture of the cell.

It is obvious that during overcharge: (i) more lithium-ions transfer from cathode to anode and if the anode does not have enough room to accommodate them, metallic lithium deposition may occur, (ii) the electrolyte decomposes and produces gaseous substances, and (iii) dissolution of transition metals (e.g., Co, Ni, etc.) occurs at the cathode. These metals transfer to the anode and cause soft shorting in combination with the deposited lithium metal.

The use and advantages of a carbon fiber composite as an anode material was disclosed by Hossain [10] in 2002 and is now considered one of the more effective high capacity anode materials for lithium-ion batteries [11–14]. The intercalation of lithium into carbon fiber through copper [15] and silver [16] films has also been reported by Takamura and co-workers. The physical properties of carbon fiber composite minimize the side-reactions that generate heat during overcharge. The low surface area, high thermal conductivity, absence of PVDF binder, the copper substrate (with the resulting absence of a thermal gradient) and the low coefficient of thermal expansion are some of the advantages. It has been shown from differential scanning calorimetry (DSC) [17] and accelerated rate calorimetry measurements [18] that carbon fiber composite generates much less heat than mesophase carbon microbeads (MCMB). As an additional advantage, a carbon fiber composite does not contain any inactive material (no binder or metal substrate). The entire composite electrode provides active sites for lithium-ion intercalation. This excess capacity of the composite anode [12], due to the absence of a copper substrate and binder, can be utilized to accommodate more lithium ions during overcharge.

This paper describes overcharge studies of prototype 5.5 Ah lithium-ion pouch cells made with carbon fiber composite anodes and the subsequent analysis of the components of the overcharged cells.

## 2. Experimental

Several prismatic design prototype lithium-ion pouch cells were made with carbon fiber composite anodes, $LiCoO_2$ cathodes and with 1.4 M $LiPF_6$ in a mixture of ethylene carbonate (EC) and ethyl methyl carbonate (EMC) as the electrolyte. The carbon fiber composite was made from pitch-based carbon fibers heat-treated to 2850 °C under an inert atmosphere. The thickness of the composite was $140 \pm 5$ μm. The cell configuration was as follows:

C/2/S/A/S/C/S/A/S—/C/S/A/S/C/2

where C/2 is the single-sided cathode, S the polyethylene separator (Tonen Chemical Corporation), A the carbon fiber composite anode, and C is the double-sided cathode. The total number of electrodes used for the development of the cells were C/2 = 2, C = 9, and A = 10. The dimensions of the anodes were 115 mm × 80 mm and those of the cathodes were 112 mm × 77 mm. The thickness of the separator was 25 μm.

The carbon fiber composite electrodes were bagged with the separator. The bagged negative electrodes were then sandwiched in between positive electrodes. The positive electrode tabs were welded. Similarly, the negative electrode tabs were also welded. The resistance between the positive electrodes and the negative electrodes was measured to insure that the stack was not electrically shorted.

The electrode stack assembly was then placed in between three-layer packaging material (plastic foil/Al foil/plastic foil) and was sealed firstly on three sides of the stack excluding the side opposite to the electrode tabs. The sealed stack was then evacuated and filled with a measured amount of 1.4 M $LiPF_6$ electrolyte. The cell was then fully sealed. All of these operations were carried out in a glove box ($H_2O < 1$ ppm). The seal of the plastic bag was checked several times prior removal from the glove box for electrochemical measurements.

The ratios of anode to cathode capacities (A/C) used in the cells were either 1.1 or 1.0 based on the specific capacities of the carbon fiber composite anode and the $LiCoO_2$ cathode which were 300 and 140 mAh $g^{-1}$, respectively. The higher anode to cathode capacity ratio is feasible in these practical lithium-ion cells due to the replacement of several inactive components (the copper substrate and binder) by anode material, which in turn, allows the anode to accommodate more lithium ions during overcharge and thus avoid deposition of metallic lithium.

A representative cell is shown in Fig. 1. The cells weigh approximately 105 g and their dimensions are 150 mm × 95 mm × 4.5 mm. The as-assembled uncharged open-circuit voltages (OCVs) of the prototype pouch cells were in the range of 5–30 mV. The pouch cells were "formed" using


Fig. 1. Picture of a 5.5 Ah lithium-ion cell made with carbon fiber composite anode, $LiCoO_2$ cathode, and 1.4 M $LiPF_6$ in EC/EMC (1:3, v/v).

an Arbin Model BT 2043 (ABTS 4.0) cycler according to the following procedure:

The cells were first charged at a constant current of 700 mA to 4.2 V and then at a constant voltage (4.2 V) for a period of 3 h or until the residual current dropped to 70 mA. After charge, the cells were kept at their open-circuit voltages for 5 min and then discharged at a constant current of 700 mA to a cut-off voltage of 3.0 V. The charge–discharge process was continued two to three times in order to obtain a fairly consistent value of the charge–discharge capacity.

Fig. 2 represents the first charge–discharge profiles of a cell. The first charge capacity of the cell was 5.96 Ah and the corresponding discharge capacity was 5.48 Ah, indicating an irreversible capacity loss of only 8%. In the subsequent two cycles, a rapid drop in residual current was observed during the constant voltage step of the charge process and also a slight increase in the discharge capacity with almost zero irreversible capacity loss.

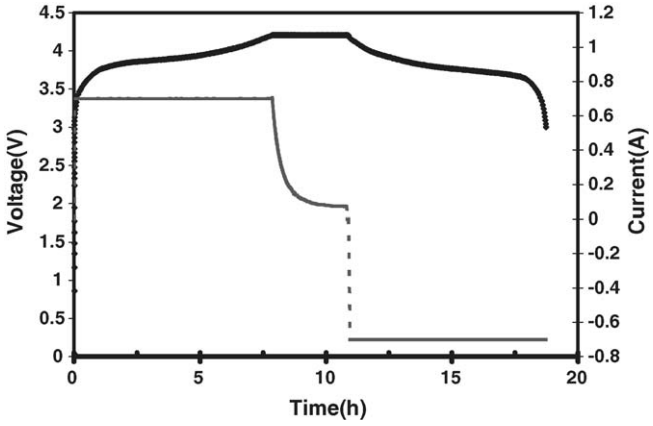


Fig. 2. First charge–discharge profiles of a 5.5 Ah lithium-ion cell.

The "formed" cells were first used to examine the charge profiles at different rates and then to evaluate deliverable capacity, specific energy and energy density, rate capability, and finally for overcharge studies.

Scanning electron microscopy (SEM—model AMRAY 1860 FE) and X-ray fluorescence spectroscopy (XRF—model TRACOR Xray Spectrace 5000) techniques were used to examine and analyze the surface morphology of unused and overcharged cell components and also the cobalt-content of the cathodes and anodes.

## 3. Results and discussion

### 3.1. Charge profiles

The charging characteristics of the developed lithium-ion cells have been investigated at different rates. Fig. 3 shows the charging profiles of a representative cell. If the cell is charged at the 1*C* rate, the cell can attain over 85% charge capacity in 1 h, over 90% in 1.5 h, and over 98% in 2 h. On the other hand, if the cell is charged at the *C*/3 rate, it can attain 65% capacity in 2 h and over 95% capacity in 3 h. These results are comparable to those observed from commercial cells.

### 3.2. Capacity, specific energy, and energy density

Prior to exposure to overcharge, the discharge capacity of the cells was measured at a1. 8 A (*C*/3) current drain and the specific energy (Wh $kg^{-1}$) and energy density (Wh $l^{-1}$) of the cells were calculated to ensure that the cells were healthy and that the exposed surface area of the cells was not large (compactness of the cell). Fig. 4 represents the discharge behavior of four representative cells. All four cells delivered a capacity >5.5 Ah at ambient temperature with an average operating voltage of 3.78 V.

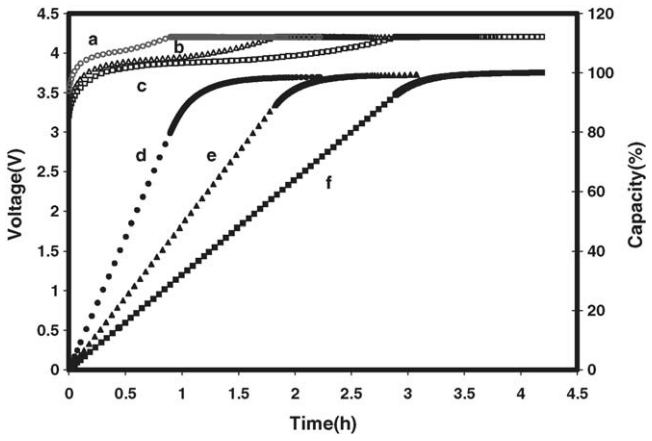


Fig. 3. Charge profiles of a representative cell. (a) Voltage at 5.00 A, (b) voltage at 2.75 A, (c) voltage at 1.80 A, (d)-capacity at 5.00 A, (e) capacity at 2.75 A, and (f) capacity at 1.80 A.

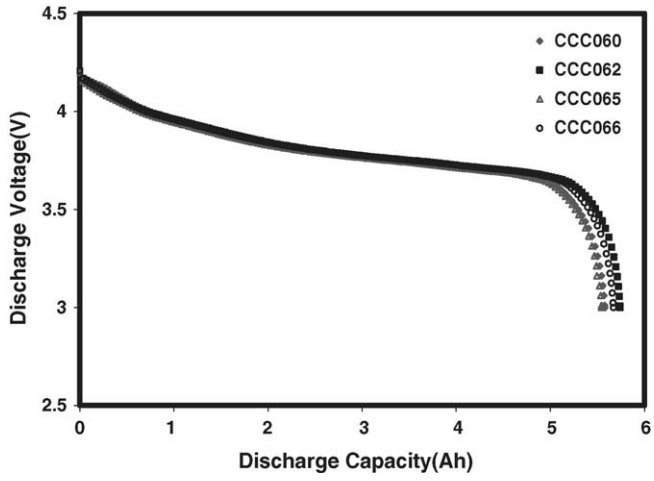


Fig. 4. Discharge behavior of four lithium-ion cells at 1.8 A.

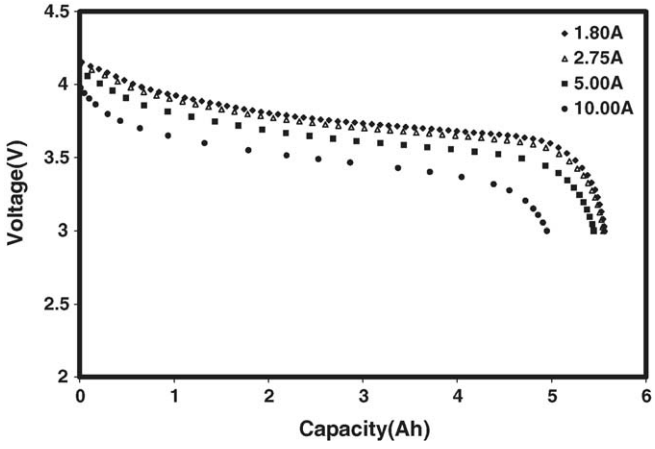


Fig. 5. Delivered capacity at different current drains of a representative cell.

The specific energies and energy densities of these cells are tabulated in Table 1. The cells delivered an average specific energy and energy density of 200 Wh $kg^{-1}$ and 330 Wh $l^{-1}$, respectively.

### 3.3. Rate capability/Ragone plot

The rate capability of a representative cell (CCC060) was examined and is shown in Fig. 5. The cell delivered a capacity of 5.56 Ah at 1.8 A (∼*C*/3) current drain. When the cell was discharged at 5 A (∼1*C*), the cell delivered 5.45 Ah 98% of *C*/3 rated capacity. At ∼2*C* rate (10 A), the cell delivered 4.96 Ah capacity—almost 90% of *C*/3 rated capacity.

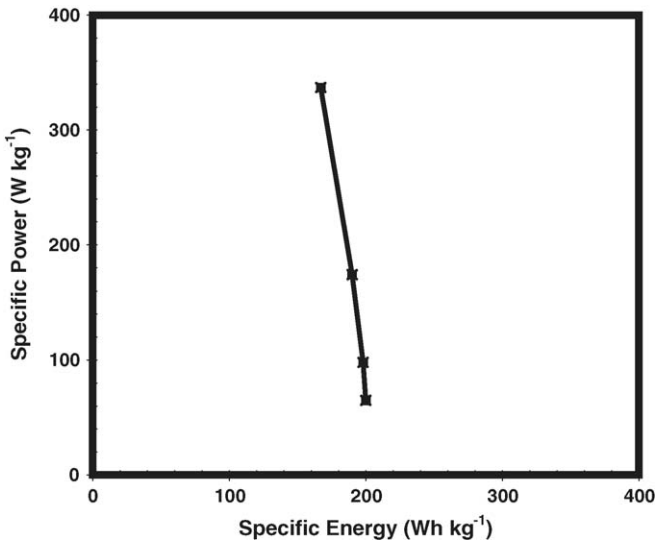


Fig. 6. Ragone plot of a lithium-ion cell made with carbon fiber composite anode.

The cells are designed for delivering high energy and moderate power. Fig. 6 shows Ragone data obtained under constant power discharge conditions. The cell delivers a specific energy of 167 Wh $kg^{-1}$ with a specific power of 337 W $kg^{-1}$.

### 3.4. Overcharge studies

After evaluating the health status of the 5.5 Ah cells, overcharge studies of these cells were carried out at 5.0 A (1*C*). The results are described below:

#### 3.4.1. Cell with A/C = 1.1

A representative 5.5 Ah cell (CCC060) was connected to a voltammeter and also to a 24-channel Arbin cycler. The body temperature of the cell was measured with a thermocouple. The open-circuit voltage (OCV) and temperature ($T_1$) of the cell prior to charge/overcharge were 3.265 V and 25.1 °C, respectively. A plastic plate and a steel slab of approximately 4 kg in weight were placed on top of the cell prior to the start of charging/overcharging in order to avoid separation of anodes and cathodes due to expansion during overcharge.

The upper voltage limit of the channel used for charging/overcharging the cell was set to 12.0 V. The cell was then charged and overcharged at 5.0 A (∼1*C* rate). During overcharge, no significant change in temperature (29.2 °C) and structural integrity of the cell was observed up to 5.0 V.

Table 1
Delivered specific energy and energy density of lithium-ion cells at 1.8 A

| Cell no. | Weight (g) | *A*/*C* capacity ratio | Dimension (mm) | Discharge capacity (Ah) | Average voltage (V) | Specific energy (Wh $kg^{-1}$) | Energy density (Wh $l^{-1}$) |
|---|---|---|---|---|---|---|---|
| CCC060 | 104 | 1.1 | 150 × 95 × 4.5 | 5.56 | 3.75 | 200 | 325 |
| CCC062 | 106 | 1.1 | 150 × 95 × 4.5 | 5.74 | 3.76 | 204 | 336 |
| CCC065 | 102 | 1.0 | 150 × 95 × 4.5 | 5.54 | 3.78 | 205 | 327 |
| CCC066 | 103 | 1.0 | 150 × 95 × 4.5 | 5.59 | 3.78 | 204 | 330 |

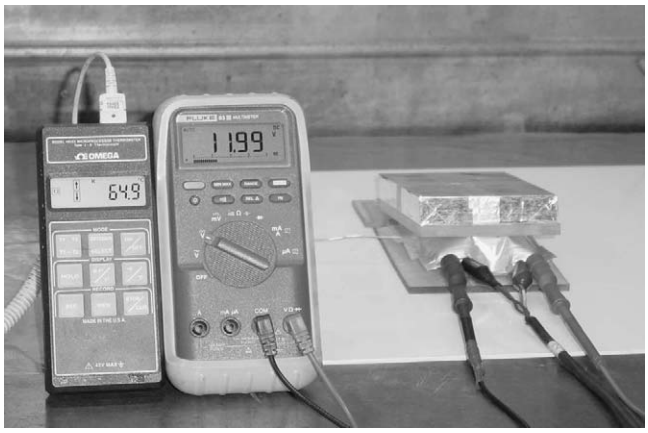

Fig. 7. Cell voltage and temperature during overcharge at 1*C* rate.

When the cell voltage reached to 6.65 V, a significant expansion of the cell packaging was observed due to gas generation inside the cell caused by electrolyte decomposition. The body temperature of the cell increased to 42.2 °C. The cell voltage then increased sharply to 11.99 V (the set up voltage limit) and the cell became a balloon even with a weight of 4 kg on top of it as shown in Fig. 7. The temperature of the cell increased to 64.9 °C ($T_2$). The change in temperature ($\Delta T = T_2 - T_1$) of the cell due to overcharge at the 5 A (∼1*C*) rate was approximately 40 °C.

Fig. 8 shows the voltage and temperature responses of the cell during charge/overcharge at a constant current of 5.0 A (∼1*C*) until the cell voltage reached the upper set up limit of the channel (12 V). The cell was then programmed to stay at a constant voltage (12 V) until the current dropped to 50 mA.

### 3.4.2. *Cell with A/C = 1.0*

The arrangement and procedure to perform the overcharge test of a cell with A/C equal to 1.0 was the same as described above for the cell with A/C = 1.1. The overcharge test of the cell was initially at a cell temperature of 18 °C. The voltage, temperature, and current responses during charge/overcharge at 5 A (∼1*C*) are shown in Fig. 9. The change in cell body temperature ($\Delta T$), in this case, was approximately 60 °C, which was

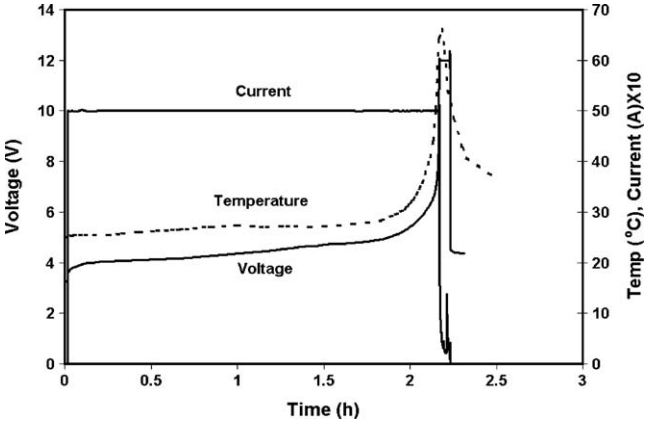


Fig. 8. Voltage, temperature, and current responses during charge-overcharge of a lithium-ion cell (A/C = 1.1) at 1*C* rate.

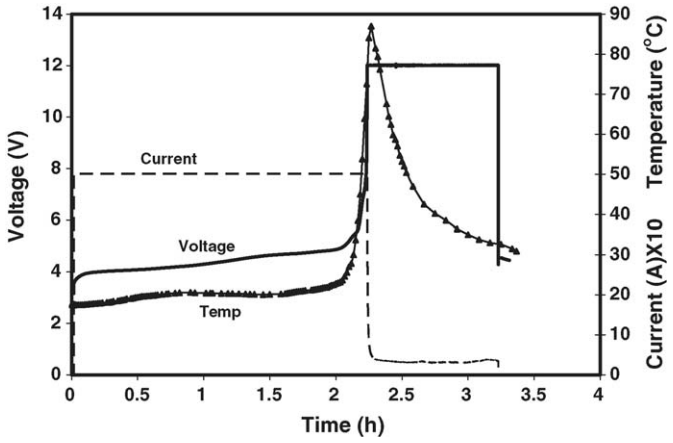


Fig. 9. Voltage, temperature, and current responses during charge-overcharge of a lithium-ion cell (A/C = 1.0) at 1*C* rate.

20 °C higher than that observed with the cell where A/C was 1.1.

During overcharge, for both the cases, the cell voltage rose monotonically to 5.0 V and then at a higher rate and finally sharply hit the voltage limit of 12 V. Lithium-ion transfer was the dominant process initially with a contribution from solvent decomposition for voltages above 5.0 V. There was no fire, smoke, or explosion.

It is not clear what causes the 5.5 Ah carbon fiber composite-based lithium-ion pouch cells to generate relatively low heat during overcharge at the 1*C* rate. It could be related to the favorable physical properties of the composite anode, such as low surface area [2,4], absence of PVDF binder [3,8], and copper substrate (with absence of thermal gradient), high thermal conductivity [19], or a low coefficient of thermal expansion. From the overcharge test results, it is clear that a slightly higher anode to cathode capacity ratio leads to a lower heat generation during

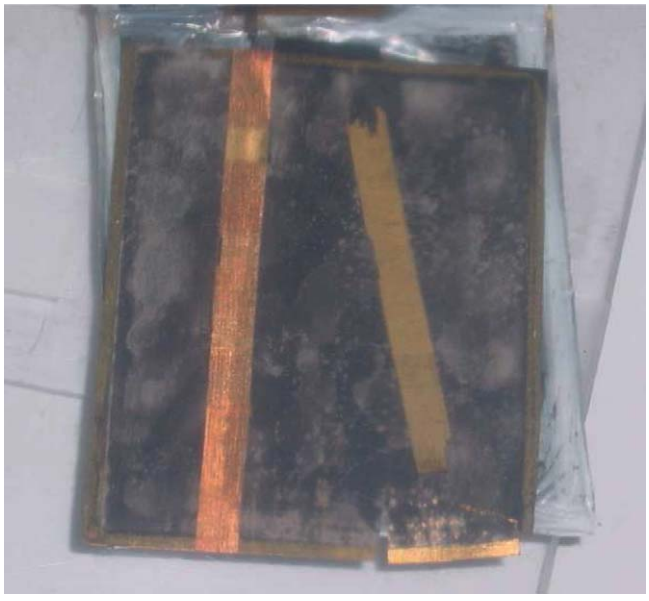

Fig. 10. Picture of overcharged carbon fiber anode. A small strip was peeled off to expose a portion of the bulk anode.

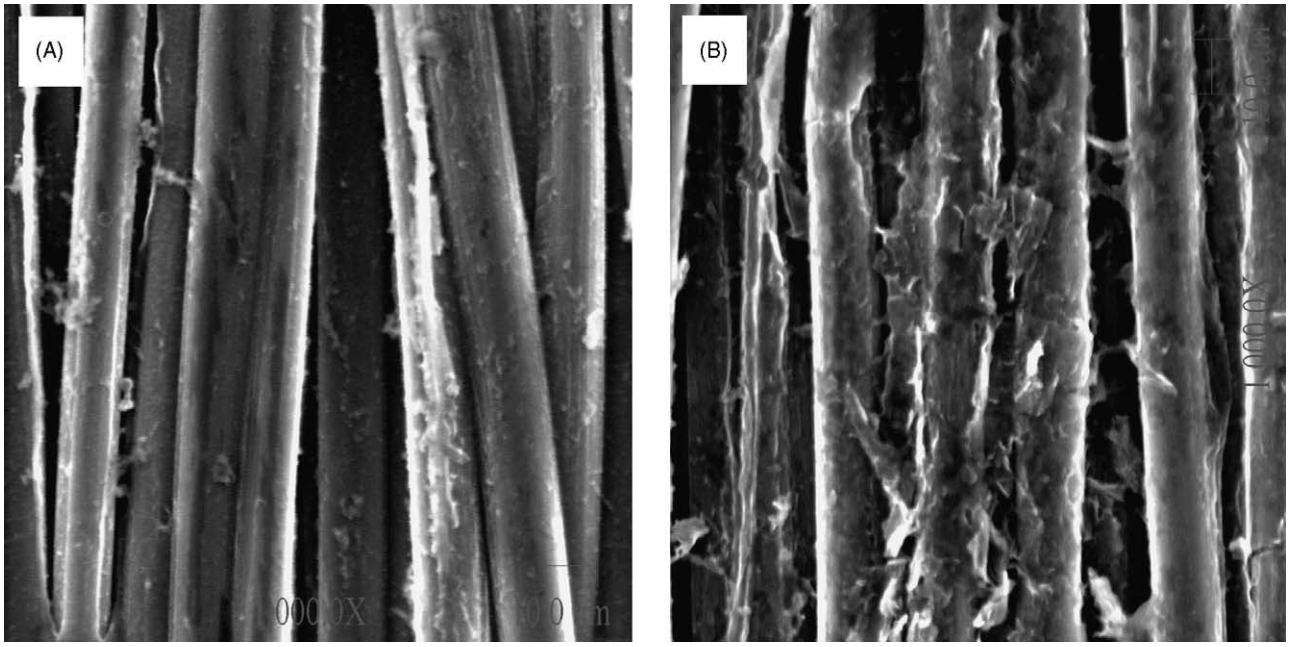


Fig. 11. SEM images of (A) unused and (B) overcharged carbon fiber anodes.

overcharge. It is the use of a carbon fiber composite anode that allows the use of a higher anode to cathode capacity ratio without sacrificing performance (cycle life, rate capability, specific energy, etc.).

The approach of using a higher anode to cathode capacity ratio could be implemented to address the overcharge related safety issues with presently used commercial carbon anodes. However, the implementation of such an approach would not only lower the specific energy and energy density, it would also affect the cycle life and rate capability [17] of the resulting cells.

### 3.5. Analysis of overcharged cell components

The overcharged cell was carefully degassed and transferred to an inert atmosphere where the cell was dissected to analyze each of the cell components. The electrode stacks of the overcharged cells were found to be tightly bonded and no separation of anodes from cathodes was observed.

#### 3.5.1. Carbon fiber composite anode

Fig. 10 shows a picture of the overcharged carbon fiber composite anode. A layer of unknown black material (probably cobalt compounds) was found on the fully lithiated overcharged anode. The bulk of the overcharged anode was a golden color ($LiC_6$) as shown in the picture (a small strip was peeled off to expose a portion of the bulk anode). The extra part of the carbon fiber composite anode (the anode was slightly bigger than the cathode) was also found to be fully lithiated (golden color).

The mechanical strength of the composite anode exposed to overcharge was found to be much weaker than that of a fresh carbon fiber composite anode. The overcharged anode was washed in isopropyl alcohol several times to remove the electrolyte salts and completely de-lithiate it. It was then dried in a vacuum oven. In this study, no attempt was made to analyze the soluble reac-

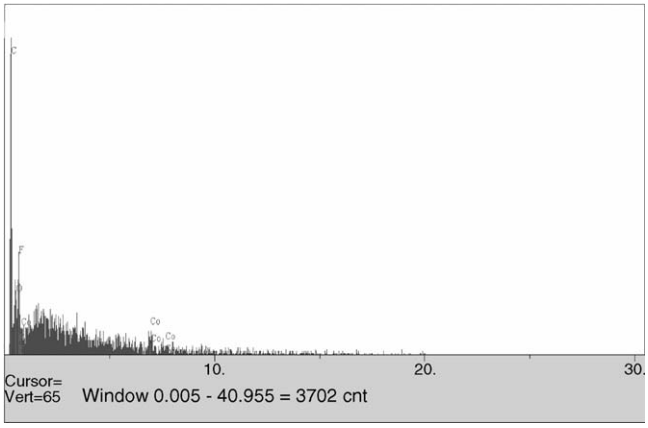


Fig. 12. EDX analysis of overcharged anode shows presence of cobalt.

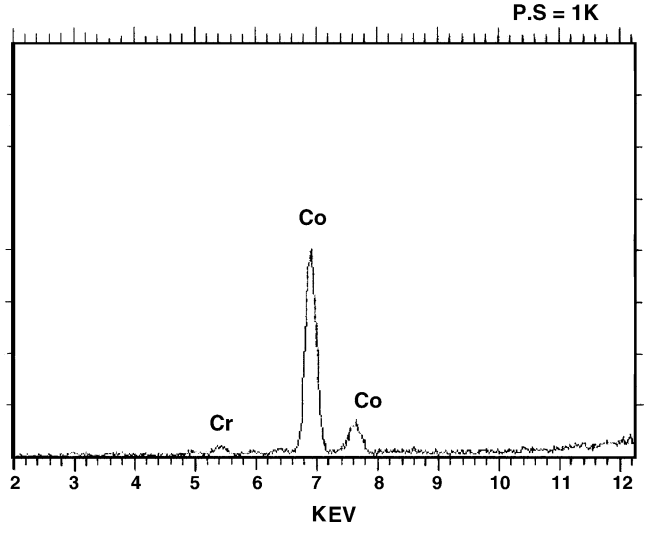


Fig. 13. XRF analysis of overcharged anode shows presence of cobalt.

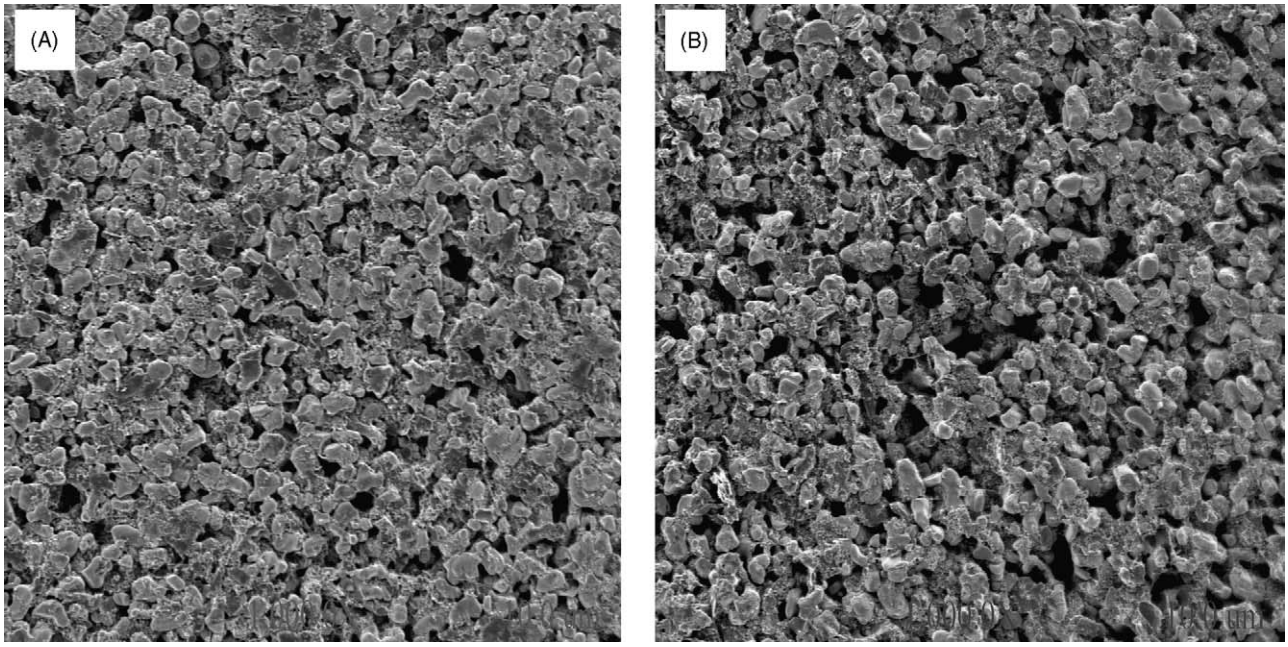


Fig. 14. SEM images of (A) unused and (B) overcharged cathode.

tion products from the solvent decomposition. The morphology of the overcharged anode was then examined using a scanning electron microscopy. The SEM images of the fresh and the overcharged anodes are shown in Fig. 11. It is evident from the morphology that the bonding between the carbon fibers of the composite anodes of overcharged cells is weaker than that of the fresh carbon fiber composite. The phenolic resin matrix, which is used to produce the carbon fiber composite and which converts to amorphous carbon on heat-treatment, was not able to hold the carbon fibers during overcharge of the anode.

The EDX (Fig. 12) and XRF (Fig. 13) analyses indicated the presence of cobalt (Co) on the overcharged composite anode, which must have transferred from the $LiCoO_2$ cathode during overcharge. In Fig. 13, a small peak of chromium (Cr) was also observed which is one of the common impurities in most commercial $LiCoO_2$ cathode materials. The dissolution of cobalt from a $LiCoO_2$ cathode due to higher voltage (4.5 V) cycling and the evidence of cobalt deposition on the anode were also observed by Tarascon and co-workers [20].

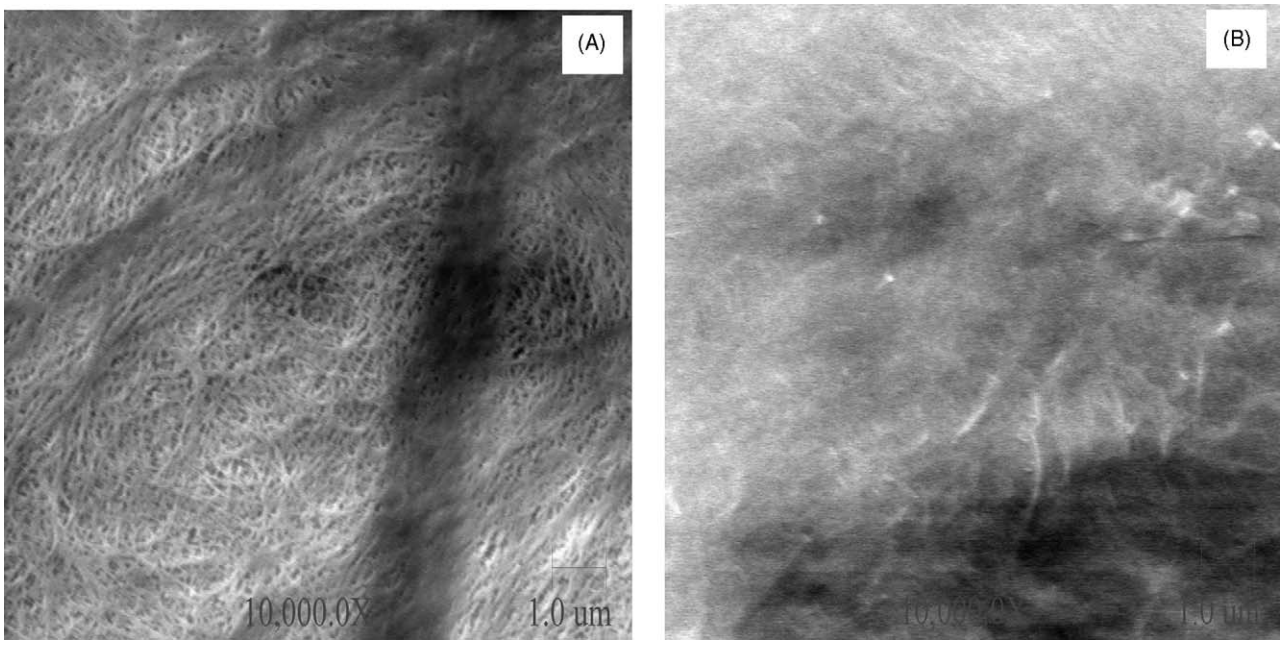


Fig. 15. SEM images of (A) unused and (B) overcharged separator.

*3.5.2. Lithium cobalt dioxide cathode*

The SEM images (Fig. 14) show no apparent change in the morphology of unused and overcharged lithium cobalt dioxide cathodes. However, the cathode materials peeled off easily from the Al-substrate of the overcharged cathode. Thus overcharge reduces the adhesion of the cathode material to the substrate.

The loading of cobalt in the overcharged cathode was determined using the XRF technique. The cobalt loading was 12.3 mg $cm^{-2}$ as compared to 12.8 mg $cm^{-2}$ for an unused cathode. The loading of cobalt in the cathode of a cell which was cycled over 50 cycles in the voltage range of 4.2–3.0 V and never exposed to an overcharge voltage (>4.2 V) was also determined. The loading of this cathode was 12.7 mg $cm^{-2}$, almost the same as that of an unused cathode. These findings confirm that cobalt dissolution occurs from the cathode during overcharge.

*3.5.3. Separator*

Surface images of the unused separator and the separator obtained from the overcharged cell are shown in Fig. 15. The porous structure of the unused separator is clearly visible whereas the pores are not seen in the separator of the overcharged cell. The carbon fiber composite-based lithium-ion cells generate relatively low heat during overcharge (only 65 and 87 °C body temperatures for the cells with A/C = 1.1 and 1.0, respectively—inside temperature may be 25–35 °C higher than the body temperature). The inside heat generated is sufficient to soften, shrink, and collapse the pores of the polyethylene separator as shown in Fig. 15 (B). Due to collapse of these pores, the flow of current ceases, and the voltage rises sharply to 12 V (see Figs. 8 and 9), during overcharge but without causing any smoke, fire, or explosion.

## 4. Conclusions

Carbon fiber composite-based prototype 5.5 Ah lithium-ion pouch cells delivered high specific energy (200 Wh $kg^{-1}$) with a high anode to cathode capacity ratio (1.1). The cells generated low heat during overcharge at a relatively high (1*C*) rate. The generation of a relatively low heat during overcharge may be related to the physical characteristics of the carbon fiber composite anode. The high anode to cathode capacity ratio that the carbon fiber composite anodes can offer to the cells also lowers the heat generation during overcharge. It is believed that enough heat is generated at relatively low temperatures to collapse the porous structure of the separator and thus initiate an automatic shutdown mechanism that blocks current flow and prevents fire or explosion during overcharge.

## Acknowledgment

Financial support provided by DOE, Office of Science, contract number DE-FG03-01ER83280/A002 is gratefully acknowledged.

## References

[1] U. von Sacken, E. Nodwell, A. Sundher, J.R. Dahn, Solid State Ionics 69 (1994) 284.
[2] M.N. Richard, J.R. Dahn, J. Electrochem. Soc. 146 (6) (1999) 2068–2077.
[3] H. Maleki, G. Deng, A. Anani, J. Howard, J. Electrochem. Soc. 146 (9) (1999) 3224–3229.
[4] D.D. MacNeil, D. Larcher, J.R. Dahn, J. Electrochem. Soc. 146 (10) (1999) 3596–3602.
[5] T.D. Hatchard, D.D. MacNeil, A. Basu, J.R. Dahn, J. Electrochem. Soc. 148 (7) (2001) A755–A761.
[6] F. Joho, P. Novak, M.E. Spahr, J. Electrochem. Soc. 149 (8) (2002) A1020–A1024.
[7] D.D. MacNeil, J.R. Dahn, J. Electrochem. Soc. 148 (11) (2001) A1205–A1210.
[8] Ph. Biensan, B. Simon, J.P. Peres, A. de Guibert, M. Broussely, J.M. Bodet, F. Perton, J. Power Sources 81–82 (1999) 906.
[9] R.A. Leising, M.J. Palazzo, E.S. Takeuchi, K.J. Takeuchi, J. Electrochem. Soc. 148 (8) (2001) A838–A844.
[10] S. Hossain, U. S. Patent 6,436,576 B1, August 2002.
[11] S. Hossain, Y. Saleh, R. Loutfy, J. Power Sources 96 (2001) 5–13.
[12] S. Hossain, Y.-K. Kim, Y. Saleh, R. Loutfy, J. Power Sources 114 (2003) 264–276.
[13] M.C. Smart, S. Hossain, B.V. Ratnakumar, R. Loutfy, L.D. Whitcanack, Proceedings 42nd Power Sources Conferences, June 12–15, 2006.
[14] S. Hossain, R. Loutfy, Y.-K. Kim, Y. Saleh, J.P. Thomas, M.T. Keennon, Proceedings 41st Power Sources Conference, 2004, pp. 282–285.
[15] J. Suzuki, M. Yoshida, C. Nakahara, K. Sekine, M. Kikuchi, T. Takamura, Electrochem. Solid-State Lett. 4 (1) (2001) A1–A4.
[16] J. Suzuki, O. Omae, K. Sekine, T. Takamura, Solid State Ionics 152–153 (2002) 111–118.
[17] S. Hossain, Y. Kim, Y. Saleh, R. Loutfy, 17th Annual Battery Conference, Long Beach, California, January 15–18, 2002.
[18] S. Hossain, Y.-K. Kim, Y. Saleh, R. Loutfy, The 23rd International Battery Seminar & Exhibit, Fort Lauderdale, Florida, March 13–16, 2006.
[19] H. Maleki, J.R. Selman, R.B. Dinwiddie, H. Wang, J. Power Sources 94 (2001) 26–35.
[20] G.G. Amatucci, J.M. Tarascon, L.C. Klein, Solid State Ionics 83 (1996) 167–173.